Complex crystal structures of Te-II and Se-III at high pressure

C. Hejny and M. I. McMahon
School of Physics and Centre for Science at Extreme Conditions, The University of Edinburgh, Mayfield Road, Edinburgh, EH9 3JZ, United Kingdom

(Received 6 June 2004; published 12 November 2004)

Te-II, the high-pressure phase of tellurium stable between 4 and 7 GPa, is found to have a triclinic structure that is previously unknown in the elements, but which is closely related to the incommensurate Te-III structure. Se-III is found to be isostructural with Te-II. The appearance of additional weak reflections in Te-II profiles below 4.3(1) GPa suggests the existence of a previously unknown phase which might be related to Se-II.

DOI: 10.1103/PhysRevB.70.184109 PACS number(s): 61.50.Ks, 62.50.+p

Te-I, the stable phase of tellurium at ambient conditions, has a trigonal crystal structure comprising infinite helical chains running parallel to the *c* axis and which is only slightly distorted from that of primitive cubic. Under pressure, Te-I transforms to Te-II,[1–4] which is stable from 4 to 7 GPa[5–8] and which is metallic in contrast to the semiconducting behavior of Te-I.[9,10] Te-II is also a superconductor, with a superconducting transition temperature that is strongly pressure dependent.[11,12]

The structure of Te-II is known to be complex,[13] and has long been reported as monoclinic ($a=3.104$ Å, $b=7.513$ Å, $c=4.760$ Å, $\beta=92.71°$) with 4 atoms per unit cell and a structure comprising puckered layers that contain zig-zag chains with alternating long and short bonds.[13] The space group of this structure has most recently been determined as $P2_1$.[8] The zig-zag chains are reported to be retained in the higher-pressure Te-III phase, where β becomes 90° and the unit cell is therefore orthorhombic.[13] The high-pressure structures of Se-III and Se-IV are reported to be isostructural with Te-II and Te-III, respectively. However, in their recent detailed study of Te-Se alloys, Ohmassa *et al.*[8] noted that diffraction profiles of Te-II at 6 GPa contained additional reflections not accounted for by the reported monoclinic structure, and noted that this might indicate that the true unit cell of Te-II was some three times larger than previously reported.

Recently, we have shown that rather than having the structures reported previously,[5,8,13,14] Te-III has a monoclinic structure that is incommensurately modulated, with a *q* vector that is strongly pressure dependent, and which reaches a maximum value of 0.314 at pressures just above the transition from Te-II.[15] Se-IV is found to have the same incommensurate structure.[15,16] The discovery of this entirely new elemental structure type calls into question the previously reported structure of Te-II,[13] particularly in light of the extra reflections noted by Ohmassa *et al.*,[8] and raises the question as to whether the known structural complexity of Te-II might also arise because of incommensurate modulations. In order to address this possibility, we have made a detailed powder and single-crystal diffraction study of Te-II and have found it to have a commensurate triclinic structure that is closely related to that of incommensurate Te-III. Se-III is found to have the same triclinic structure.

Powder diffraction data were collected on station 9.1 at SRS, Daresbury, using an imaging plate area detector and an incident wavelength of 0.4654 Å.[17] The Te samples were finely ground powders prepared from starting material of 99.999% purity, and these were loaded into diamond anvil pressure cells using a 4:1 methanol:ethanol pressure transmitting medium. The pressure was measured using the ruby fluorescence technique,[18] and the 2*d* diffraction patterns were integrated azimuthally to give standard powder diffraction profiles.[17]

On pressure increase, diffraction peaks from Te-II were first observed at 4.0(1) GPa. However, on further compression, single-phase profiles of Te-II were not obtained before reflections from Te-III began to appear at 4.5(2) GPa. Indeed, three-phase mixtures of Te-I, Te-II, and Te-III were often observed at pressures near 4.5 GPa. Further compression increased the intensity of the Te-III peaks, and,

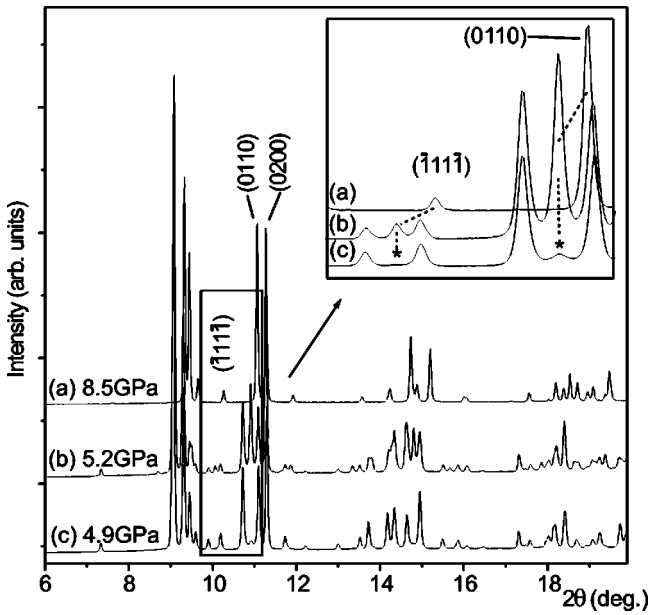

FIG. 1. Powder-diffraction profiles collected on pressure decrease from (a) single phase Te-III at 8.5 GPa, (b) a Te-II/Te-III mixture at 5.2 GPa, and (c) predominantly Te-II 4.9 GPa. The inset shows an enlarged view of the same profiles highlighting the splitting of the $(\bar{1}11\bar{1})$ and (0110) peaks of Te-III into triplets in the mixed phase regions, before becoming doublets in Te-II. Asterisks in profile (c) denote peaks from the remaining trace component of Te-III.

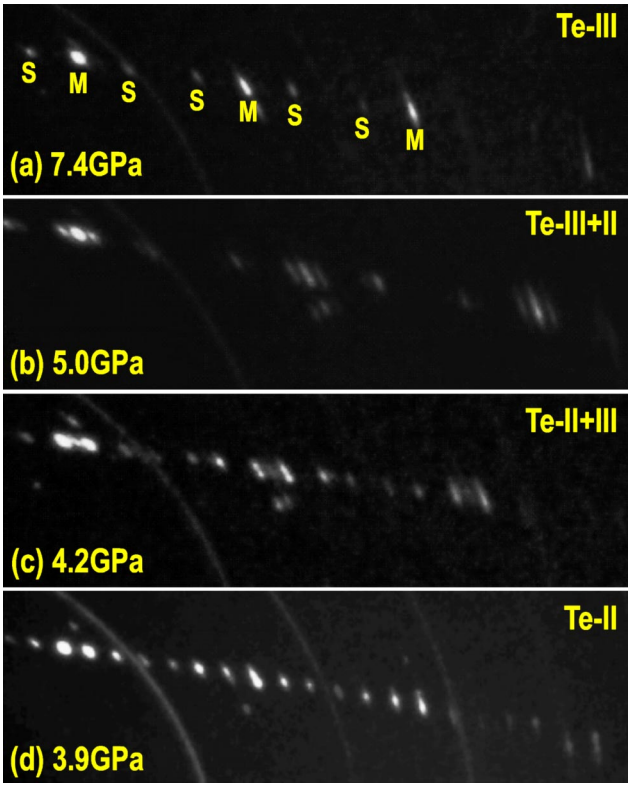

FIG. 2. Single-crystal diffraction images of Te collected on pressure decrease from (a) pure Te-III at 7.4 GPa showing the main (M) and satellite (S) reflections, (b) mixed Te-III/Te-II at 5.0 GPa, (c) predominantly Te-II at 4.2 GPa, and (d) almost single-phase Te-II at 3.9 GPa.

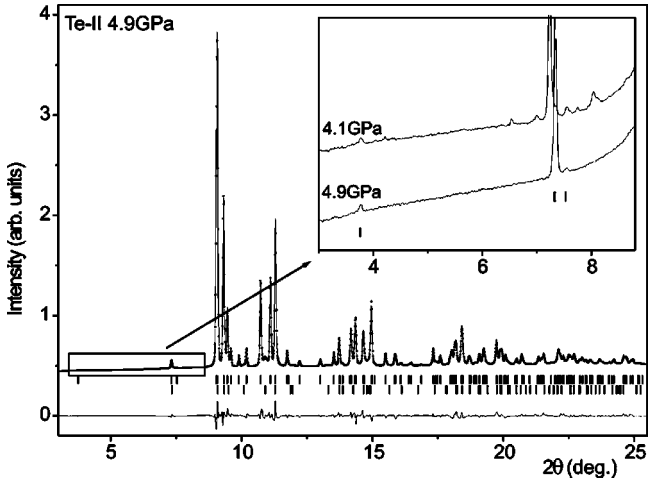

FIG. 3. Rietveld refinement of triclinic Te-II at 4.9 GPa. The upper and lower tick marks below the profile show the calculated peak positions for Te-II and the trace component of Te-III, respectively. The difference between the observed and calculated profiles is shown below the tick marks. The inset shows the additional low-angle reflections that appear in the Te-II profiles at pressures below 4.3(1) GPa.

above 8.0(5) GPa, single-phase Te-III patterns were observed [Fig. 1(a)]. On pressure decrease from Te-III, reflections from Te-II first appeared at 7.9(2) GPa, and, on further pressure decrease, increased in intensity [Fig. 1(b)]. Although further pressure decrease resulted in an almost complete transition to Te-II [Fig. 1(c)], single-phase profiles of Te-II were not observed on pressure decrease: traces of Te-III remained down to 3.8(3) GPa at which point peaks from Te-I appeared. Despite repeated attempts, we have not observed single-phase profiles of Te-II on either pressure increase or decrease; traces of either Te-I or Te-III are always present.

Comparison of the diffraction profiles from Te-III [Fig. 1(a) and Te-II (Fig. 1(c)] suggested that many of the Te-II reflections could be interpreted as originating from a splitting of Te-III reflections. This is illustrated in the inset to Fig. 1, which shows the single $(\bar{1}11\bar{1})$ and (0110) reflections of Te-III, each of which becomes a triplet in mixed phase Te-II/III profiles, before becoming a doublet in profiles from Te-II. [In fact, as is evident in profile (c) of the inset to Fig. 1, traces of Te-III are still clearly visible at 4.9 GPa, as marked by the asterisks.] The presence of these triplets, particularly those that originate from the $(\bar{1}11\bar{1})$ and (0110) reflections of Te-III, can be used to identify mixed-phase profiles. We note that the 6 GPa profile in Fig. 1 of Takumi *et al.*[14] contains such triplets, in particular that containing the (0110) reflection of Te-III, and is thus almost certainly from a mixture of Te-II and Te-III.

The splitting of the Te-III reflections at the III→II transition and the appearance of many additional reflections, in particular a low-angle reflection with a *d* spacing of 7.1 Å, suggested that Te-II has both a lower symmetry structure than Te-III and a larger unit cell. Unfortunately, attempts to index Te-II powder profiles were unsuccessful. However, the successful use of single-crystal techniques in the analysis of the structure of Te-III[15] suggested that the same sample and techniques might be used for a single-crystal study of the complex Te-II structure. Single-crystal diffraction data were therefore collected on station 9.8 at SRS, Daresbury, using the same sample and methods used for the study of incommensurate Te-III.[15]

Part of a single-crystal diffraction image from the twinned single crystal of Te-III at 7.4 GPa is shown in Fig. 2(a) from which it is easy to distinguish the main reflections (M) from the body-centered monoclinic cell from the weaker satellite reflections (S) that arise from the incommensurate modulation. When the pressure is reduced to 5.2 GPa [Fig. 2(b)], such that the sample comprises a mixture of (predominantly) Te-III and Te-II, both the main and satellite reflections split. This is more evident in Fig. 2(c) where the sample is predominantly Te-II with only a minority component of Te-III. The process is complete by 3.9 GPa [Fig. 2(d)], where the sample is almost single-phase Te-II, with only very faint traces of Te-III remaining.

Analysis of the reflection positions in Te-II at 3.9 GPa [Fig. 2(d)] relative to those in Te-III at 7.4 GPa [Fig. 2(a)] showed that they are consistent with both the α and γ angles of the monoclinic Te-III structure deviating slightly from 90° in Te-II. Te-II is thus triclinic. Furthermore, the Te-II peaks

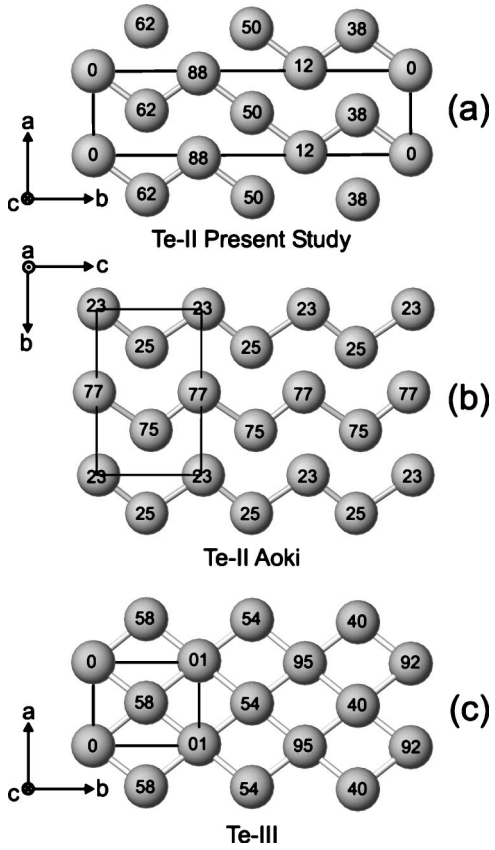

FIG. 4. (a) The structure of Te-II as viewed along the triclinic *c* axis showing the zig-zig-zag puckering of the layers. For comparison, (b) the Te-II structure of Aoki *et al.* (Ref. 13), and (c) the modulated structure of Te-III at 8.5 GPa, are also shown. In both of the Te-II structures, the nearest-neighbor distances are shown as bonds. The numbers on each atom give either the *z* [in structures (a) and (c)] or *x* [in structure (b)] coordinates in units of 0.01.

that appear on either side of the Te-III satellite peaks are not located equidistance from the satellites, which are located at $(0 \pm 0.31\ 0)$ relative to the main peaks, but rather are split equally about the $\left(0 \pm \frac{1}{3}\ 0\right)$ positions, indicating that the *b* lattice parameter of Te-II is three times larger than that of Te-III. The best fitting lattice parameters from the single crystal data at 3.9 GPa were $a=4.1$ Å, $b=14.2$ Å, $c=3.1$ Å, $\alpha=87.5°$, $\beta=112.5°$, $\gamma=91°$, and the large number of reflections evident in Fig. 2(d) can then be understood as arising from eight different twin components of Te-II: each of the two twin components of Te-III splits into a further four twins as a result of both α and $\gamma \neq 90°$.

Indexing of the Te-II powder profiles using the unit cell derived from the single-crystal data revealed that all reflections could be accounted for by a body-centered triclinic cell with $a=4.0793(1)$ Å, $b=14.1981(3)$ Å, $c=3.0977(1)$ Å, $\alpha=87.516(2)°$, $\beta=112.536(2)°$, and $\gamma=91.098(2)°$ at 4.5 GPa. Although this unit cell is nonprimitive,[19] and thus nonstandard, we have chosen to use it to describe Te-II because of its very close relationship to the (commensurate) Te-III structure obtained when the *q* vector is $\left(0, \frac{1}{3}, 0\right)$ and thus when the *b* axis of Te-III is tripled in length. This close relationship to

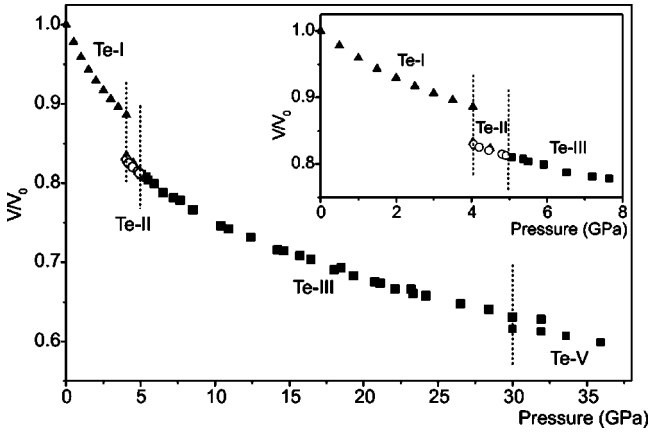

FIG. 5. The compressibility of Te to 36 GPa. The data for Te-I and Te-II plotted with closed triangles are the direct compressibility measurements of Ref. 22, and the data for Te-III and Te-V are from Ref. 16. The inset shows an enlarged view of the low-pressure region.

Te-III also provided an initial structural model for Rietveld refinement, where atoms were placed at (0,0,0), $\left(\frac{1}{2}, \frac{1}{6}, \frac{1}{2}\right)$ and $\left(0, \frac{1}{3}, 0\right)$ in space group $I1$. However, the relationship between the resulting refined atomic coordinates indicated that the structure was centrosymmetric, and so all further refinements were conducted in space group $I\bar{1}$. The final refined coordinates were (0,0,0) and (0.5310(5),0.1684(1),0.6198(5)) and the final Rietveld fit is shown in Fig. 3. The fit is excellent with $R_{wp}=5.4\%$. The structure of Te-II is entirely new in an element, and is remarkable for its triclinic symmetry—Cf is the only other element reported to have a triclinic polymorph at high pressures.[20]

The structure of Te-II as viewed along the *c* axis is shown in Fig. 4. The monoclinic structure of Te-II reported by Aoki *et al.*[13] and three unit cells of incommensurate Te-III are also shown for comparison. The structure of Te-II is clearly closely related to that of incommensurate Te-III. The III→II transition involves a tripling of the Te-III unit cell

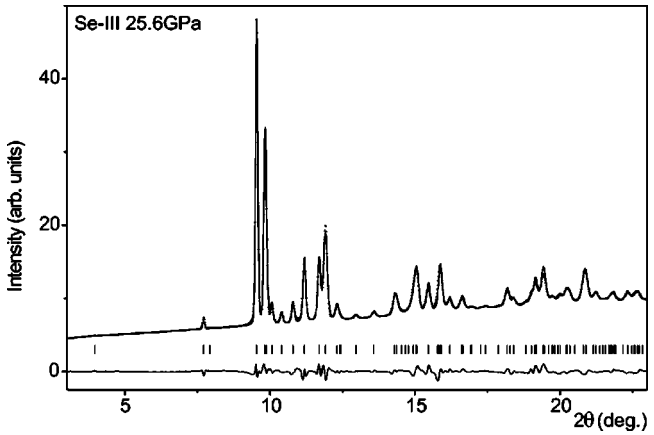

FIG. 6. Rietveld refinement of triclinic Se-III at 25.6 GPa. The tick marks below the profile show the calculated peak positions. The difference between the observed and calculated profiles is shown below the tick marks.

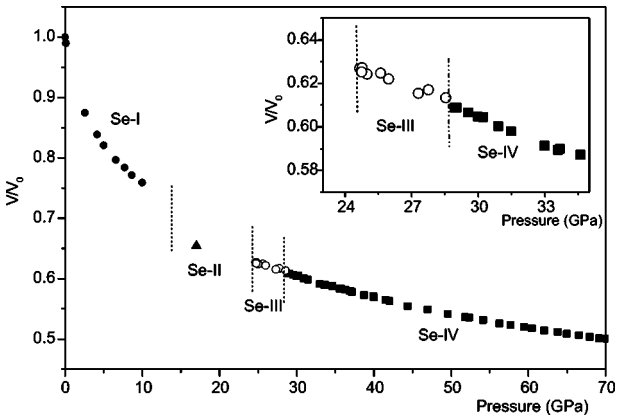

FIG. 7. The compressibility of Se to 70 GPa. The data for Se-I and Se-II are from Refs. 23 and 8, respectively. The data for Se-IV are taken from Ref. 16. The inset shows an enlarged view of the Se-III→Se-IV transition region.

along *b*, equivalent to the wave vector locking in at the commensurate value of $(0,\frac{1}{3},0)$; a slight distortion of both the α and γ cell angles of Te-III away from 90°; and a slight rearrangement of the atoms in the *ac* plane.

Although the structure of Te-II has some similarities to that proposed by Aoki *et al.*[13] [Fig. 4(b)], it differs in a number of important respects. First, Te-II is triclinic rather than monoclinic, and has six atoms per unit cell. Second, rather than the nearest-neighbor atoms being arranged in zig-zag puckered layers [Fig. 4(b)], the layers in triclinic Te-II have a zig-zig-zag puckering, similar to that reported in the C-centered monoclinic structure (space group $C2/m$) of Se-II at 17 GPa.[8] The relative stability of structures containing zig-zig-zag and zig-zag puckering has been considered by Hsueh *et al.*,[21] whose computational study of the $C2/m$ and $P2_1$ structures of Se-II and Se-III, respectively, showed that the former, with its zig-zig-zag puckering, was the more stable structure over the full pressure range investigated.

Each atom in Te-II has four nearest neighbors within the puckered layers at distances between 2.86 and 3.10 Å at 4.9 GPa, and four next-nearest neighbors in adjacent layers with two atoms at distances of 3.3–3.4 Å and a further two atoms at a distance of 3.6–3.7 Å. While the nearest-neighbor distances are very similar to the 2.80 and 3.10 Å reported by Aoki *et al.*[13] at 4.5 GPa, the spread of the next-neighbor distances is somewhat greater than in the higher-symmetry Aoki structure, where the four next-nearest atoms are all in the range 3.47–3.53 Å.

A detailed comparison of the Te-II and Te-III structures is made difficult by the incommensurate nature of Te-III, which means that the contact distances within every unit cell are different.[15] However, both the unit cells and structures of Te-II and Te-III are closely related, as discussed above and as illustrated in Fig. 4, with the six-fold coordination of Te-III arising from a reduction in the distance to the two next-nearest neighbors in the range 3.3–3.4 Å at the II→III transition. In addition, the pressure dependence of the Te-II lattice parameters over the range 4.0–4.9 GPa is such as to minimize the discontinuities found at the II→III transition: both the triclinic α and γ angles change with increasing pressure so as to approach closer to 90° at the transition; β increases so as to approach the value of 113.25° found in Te-III at 5 GPa; and the *a*, *b*/3, and *c* lattice parameters of Te-II all approach the values found in Te-III just above the transition. Although there are clear discontinuities of 2.4° and 1.0°, respectively, in the α and γ angles at the II→III transition, the volume change at the transition is too small to determine. The equation of state of Te to 36 GPa is shown in Fig. 5.

Previous studies of Te and Se have noted the similarity in the high-pressure structural behavior of these elements, and have reported that Se-III is isostructural with Te-II.[9] To confirm this we have collected diffraction data from Se-III from 24 to 29 GPa at the European Synchrotron Radiation Facility in Grenoble, using an image plate detector and an incident wavelength of 0.4176 Å. We find that Se-III does indeed have the same triclinic structure as Te-II, with lattice parameters $a=3.4648(1)$ Å, $b=12.0875(5)$ Å, $c=2.6481(1)$ Å, $\alpha=86.805(5)°$, $\beta=112.021(5)°$ and $\gamma=91.344(8)°$ at 25.6 GPa. The refined atomic coordinates in space group $I\bar{1}$ at the same pressure are (0,0,0) and (0.5393(7),0.1685(2),0.6372(7)). A Rietveld refinement of Se at this pressure is shown in Fig. 6, and the equation of state of Se to 70 GPa is shown in Fig. 7.

The structure solution of Te-II and Te-III, and the confirmation that Se-III and Se-IV are isostructural with these phases, confirms the close structural relationship of these two group-VIb elements. Given the isostructural behavior of Se and Te at higher pressures, it is intriguing that only Se has an additional high-pressure semiconducting phase—Se-II—at lower pressures. In detailed studies of Te-II on pressure decrease, however, we have noticed the appearance of additional weak reflections in the Te-II profiles that cannot be explained by the triclinic structure of Te-II (see inset to Fig. 3). These additional peaks appear reproducibly in all Te-II profiles below 4.3(1) GPa, and disappear completely if the pressure is increased again above 4.4(1) GPa. It is plausible, particularly given the similar zig-zig-zag puckering found in Se-II and Te-II/Se-III, that these peaks are associated with a previously unknown phase of Te between Te-I and Te-II that is either isostructural with, or closely related to, the structure of Se-II. However, because of the extreme weakness of the additional peaks, and the fact that other such peaks may be overlapped by the much stronger peaks of Te-II, identification of this new phase will require further work.

We acknowledge helpful discussion with Professor R.J. Nelmes. We thank Dr. M. Roberts and Dr. S. Teat of Daresbury Laboratory for setting up the 9.1 and 9.8 beamlines, Dr. M. Hanfland of the ESRF for setting up the ID09 beamline, and our colleagues Dr. J.S. Loveday and L.F. Lundegaard for help in collecting data at ESRF. This work was supported by grants from EPSRC, funding from CCLRC, and facilities provided by Daresbury Laboratory. M.I.M. acknowledges support from the Royal Society.

[1] P.W. Bridgman, Phys. Rev. **48**, 893 (1935).
[2] P.W. Bridgman, Proc. Am. Acad. Arts Sci. **74**, 21 (1940).
[3] P.W. Bridgman, Phys. Rev. **60**, 351 (1941).
[4] P.W. Bridgman, Proc. Am. Acad. Arts Sci. **74**, 425 (1942).
[5] J.C. Jamieson and D.B. McWhan, J. Chem. Phys. **43**, 1149 (1965).
[6] H.K. Mao, G. Zou, and P.M. Bell, Year Book - Carnegie Inst. Washington **80**, 283 (1980).
[7] G. Parthasarathy and W.B. Holzapfel, Phys. Rev. B **37**, 8499 (1988).
[8] Y. Ohmasa, I. Yamamoto, M. Yao, and H. Endo, J. Phys. Soc. Jpn. **64**, 4766 (1995).
[9] Y. Akahama, M. Kobayashi, and H. Kawamura, Solid State Commun. **83**, 269 (1992).
[10] I. Yamamoto, Y. Ohmasa, H. Ikeda, and H. Endo, J. Phys.: Condens. Matter **7**, 4299 (1995).
[11] I.V. Berman, Zh.I. Binzarov, and P. Kurkin, Sov. Phys. Solid State **14**, 2192 (1973).
[12] F.P. Bundy and K.J. Dunn, Phys. Rev. Lett. **44**, 1623 (1980).
[13] K. Aoki, O. Shimomura, and S. Minomura, J. Phys. Soc. Jpn. **48**, 551 (1980).
[14] M. Takumi, T. Masamitsu, and K. Nagata, J. Phys.: Condens. Matter **14**, 10609 (2002).
[15] C. Hejny and M.I. McMahon, Phys. Rev. Lett. **91**, 215502 (2003).
[16] M.I. McMahon, C. Hejny, J.S. Loveday, L.F. Lundegaard, and M. Hanfland, Phys. Rev. B **70**, 054101 (2004).
[17] R.J. Nelmes and M.I. McMahon, J. Synchrotron Radiat. **1**, 69 (1994).
[18] H.K. Mao, J. Xu, and P.M. Bell, J. Geophys. Res. **91**, 4673 (1986).
[19] The equivalent primitive unit cell is $a=7.8029$ Å, $b=7.3577$ Å, $c=7.6073$ Å, $\alpha=148.4191°$, $\beta=45.7553°$, and $\gamma=156.6577°$.
[20] R.B. Roof Jr., J. Less-Common Met. **120**, 345 (1986).
[21] H.C. Hsueh, C.C. Lee, C.W. Wang, and J. Crain, Phys. Rev. B **61**, 3851 (2000).
[22] S.N. Vaidya and G.C. Kennedy, J. Phys. Chem. Solids **33**, 1377 (1972).
[23] R. Keller, W.B. Holzapfel, and H. Schulz, Phys. Rev. B **16**, 4404 (1977).